Three-dimensional CT of the pediatric spine

Robert J. Starshak, MD; Carl R. Crawford, PhD;
Raymond C. Waisman, MD; John R. Sty, MD

We have evaluated 32 patients with a variety of spinal malformations, utilizing three-dimensional computed tomography (3D-CT). This has been useful in evaluating developmental and traumatic lesions of the pediatric spine. This is especially true if the spine is distorted by scoliosis or kyphosis. A significant advantage of 3D-CT is the ability to rotate the image in order to view the spine from different perspectives.

Drs Starshak and Sty are in the department of radiology at Children's Hospital of Wisconsin in Milwaukee; Dr Crawford is with General Electric Medical Systems in Waukesha, Wisconsin; Dr Waisman is in the department of orthopaedic surgery at Children's Hospital of Wisconsin.

It can be difficult to evaluate complex developmental or traumatic lesions of the spine with standard techniques. Historically, the mainstay in the assessment of these lesions has been plain radiographs. If these are nondiagnostic, they are often supplemented with computed tomography. Frequently, however, axial CT may be difficult to interpret, especially if the spine is grossly distorted, as with severe scoliosis or kyphosis. Prior experience with three-dimensional CT (3D-CT) in the diagnosis and treatment of complex craniofacial maladies[1,2] led us to the premise that this technology would be beneficial in studying the spine. For this reason, we undertook a study to assess the usefulness of 3D-CT in studying a variety of spinal abnormalities in children.

Materials and methods

During the period from February 1986 to October 1987, we studied 32 children

Disease Category	Anatomic Region: Cervical	Lumbar
Developmental	11	6
Traumatic	2	6
Neoplastic	2	4
Infections	0	1
Total	15	17

TABLE 1

Developmental	
Myelomeningocele	4
Torticollis	3
Klippel-Feil syndrome	3
Hemivertebrae	3
Tethered cord with lipoma	2
Diastrophic dwarfism	1
Iniencephaly	1
Traumatic	
Fracture	4
Subluxation	2
Os odontoideum	1
Postoperative complication	1
Neoplastic	
Ewing tumor	2
Osteoblastoma	2
Osteosarcoma	1
Epidural venous angioma	1
Infections	
Discitis	1

TABLE 2

A

B

*FIGURE 1. **Klippel-Feil syndrome. AP (figure 1A) and lateral (figure 1B) radiographs of the cervical and upper thoracic spine do not adequately evaluate the number and alignment of the cervical vertebrae. The spine is obscured by the mandible and the occiput. The left scapula is elevated and is rotated medially due to Sprengel's deformity.***

who had a wide variety of spinal abnormalities. These included developmental, traumatic, neoplastic, and infectious disorders (tables 1 and 2). Three-dimensional CT was performed in a retrospective fashion, if the data provided from axial CT was insufficient to completely evaluate the lesion.

Image generation

The 3D-CT images contained in this report were generated from a series of axial CT images, which were reconstructed in a field-of-view that was sufficient to include the area of interest. For lesions in the cervical region, contiguous 3-mm sections were obtained; for those in the thoracic, lumbar, or sacral regions, contiguous 5-mm sections were usually sufficient, except in small infants where 3-mm sections were required.

A mathematical representation of the surface of interest was extracted from the series of axial images by employing a special computer program. The surface of interest can be specified by selecting a threshold of CT numbers. Voxels that have a CT number greater than the threshold will be included in the resultant surface representation, while those less than the threshold will be excluded. Similarly, a range of CT numbers can be specified; voxels that have a CT number in the specified range will be included, while those out of the range will be excluded. There is a set of parameters in this computer program that describe the direction from which the image is viewed and the position of the light source that illuminates the images. Rendering the image from the mathematical representation of the surface utilizes methods that are well established in the field of computer animation. Extracting the mathematical representation of the surface of interest from the series of axial images is the most challenging portion of this problem.

An element that is critical to 3D-CT image quality is the accurate definition of the surface normal. The images contained in this paper were generated using an algorithm called "Dividing Cubes."[3] With this algorithm, it has been shown that the normalized three-dimensional gradient of

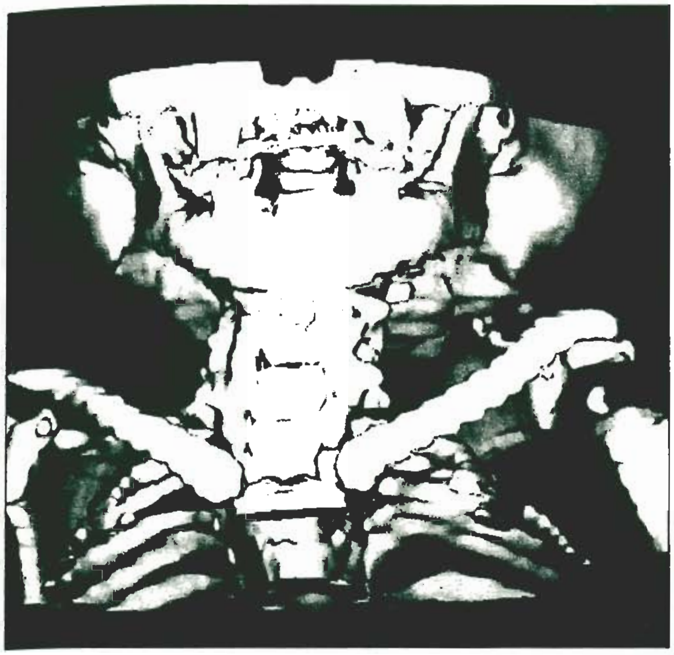

A

B

C

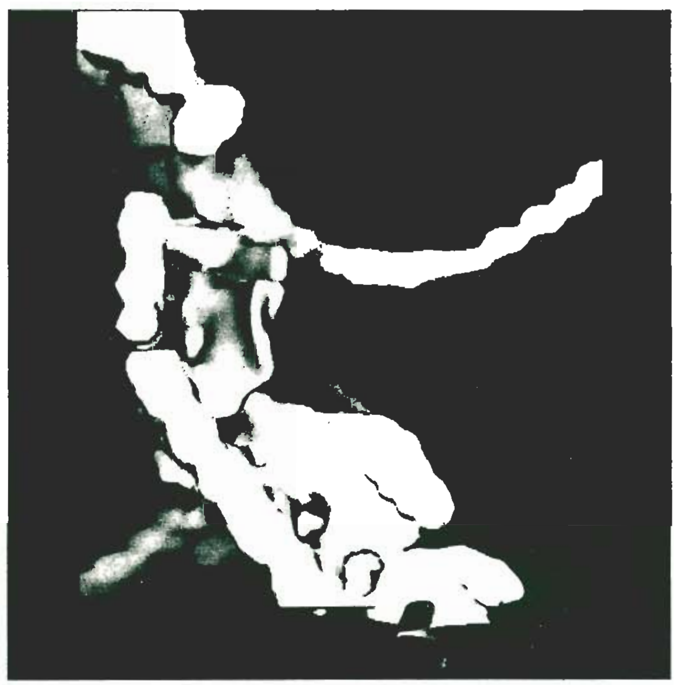

D

FIGURE 2. These three-dimensional CT images are viewed slightly from below. The anterior image (figure 2A) shows the Sprengel's deformity of the left scapula. The upper cervical vertebrae are obscured by the occiput. The posterior image (figure 2B) reveals fusion anomalies involving the posterior elements. There is spina bifida in the upper cervical region. Midline sagittal sections are viewed to the patient's left (figure 2C) and right (figure 2D), respectively. These more clearly depict the fusion anomalies involving the posterior elements. The bodies of C2 and C3 are fused into a solid block of bone. There is a rounded bony density, probably the body of C1, which is fused to the tip of the clivus. The neural foramina in the upper cervical region are abnormal in both size and orientation as a consequence of the fusion of the laminae.

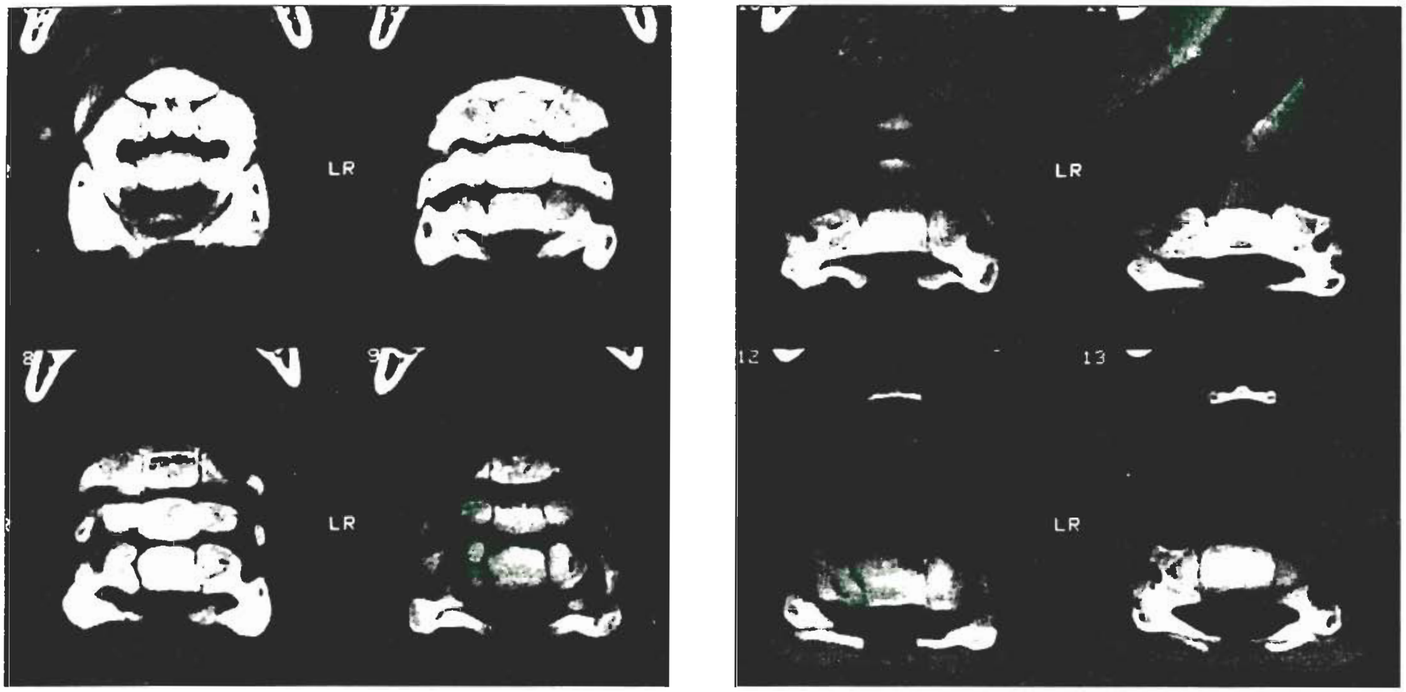

A B

FIGURE 3. ***Diastrophic dwarfism. Axial CT of the cervical spine section through the cervical vertebrae on the same axial images (figure 3A). There is severe narrowing of the AP diameter of the cervical spinal canal (figure 3B). There is spina bifida of many of the cervical vertebrae.***

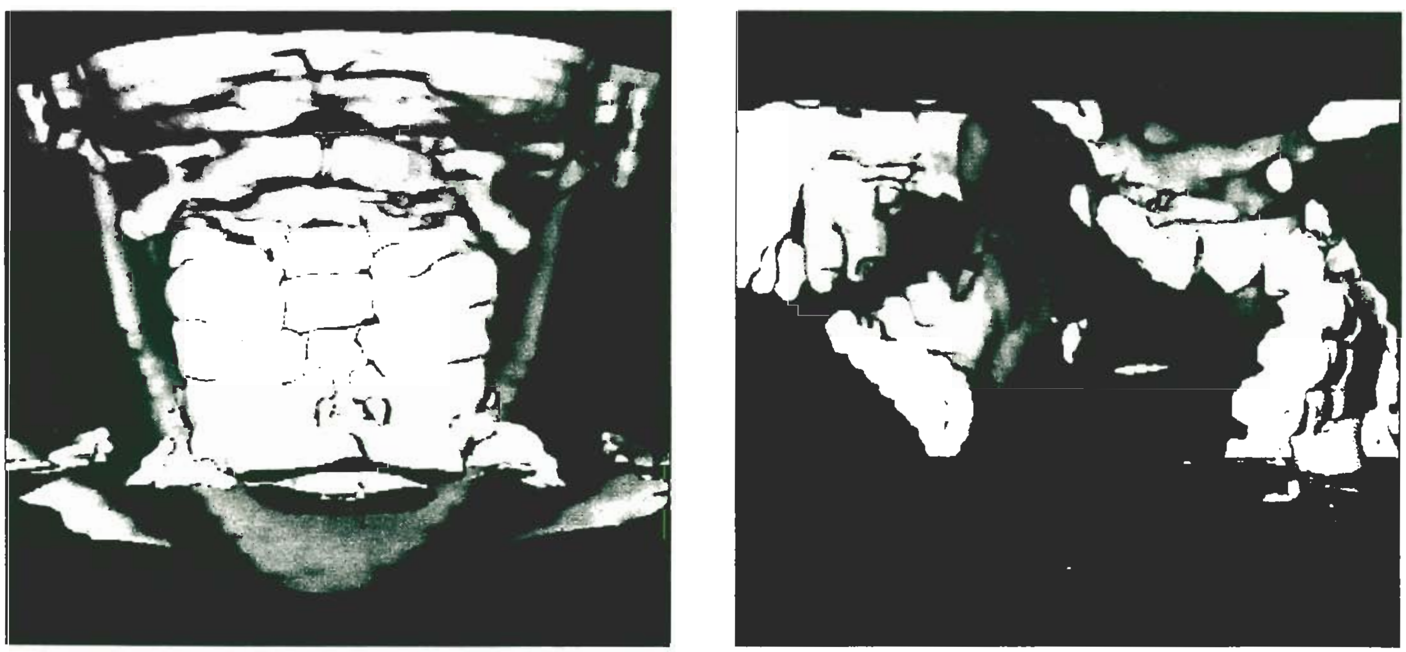

A B

FIGURE 4. ***3D-CT viewed from behind and slightly from below (figure 4A) more clearly depicts the extent of the spina bifida that involves C3 through T1. The midline sagittal section (figure 4B) is viewed slightly from below and towards the patient's right. This reveals C1 through C4 to be sharply angulated anteriorly, with respect to the remaining cervical vertebrae. The cervical spinal canal is markedly narrowed at the C4 level.***

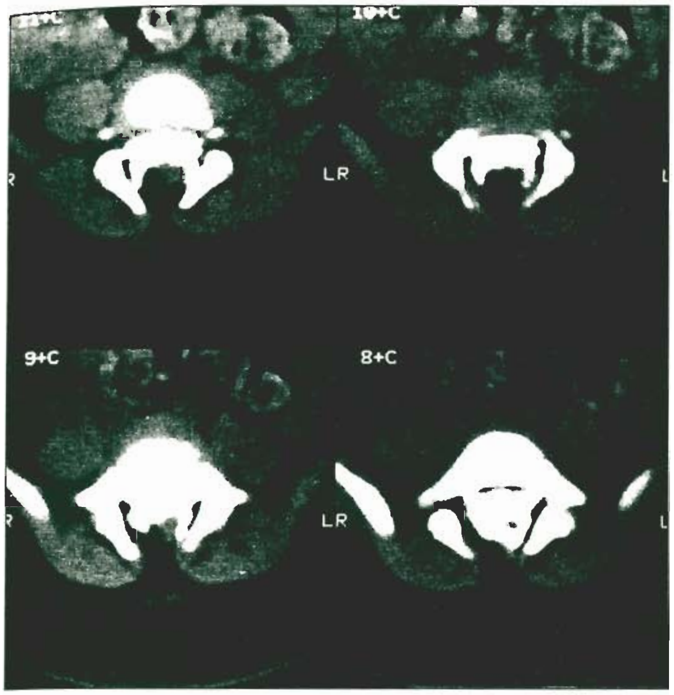

FIGURE 5. ***Tethered cord with lipoma. Axial CT following myelography (figure 5) demonstrates spinal dysraphism involving the lower lumbar spine and sacrum. The spinal cord extends to the L4 level. The thickened filum terminale lies to the left of the midline. There is fat within the spinal canal that extends posteriorly and slightly to the right to merge with the fat in the buttocks.***

A

B

FIGURE 6. ***3D-CT is viewed from behind and slightly from above (figure 6A) and the midline sagittal section (figure 6B) is viewed slightly from above and towards the patient's left. These images more clearly identify the dysraphic changes in the lower lumbar spine and sacrum. A defect is seen in the contrast-filled subarachnoid space through which the lipoma protrudes. However, the fatty nature of the mass and the tethering of the filum terminale are not apparent on the 3D-CT images***

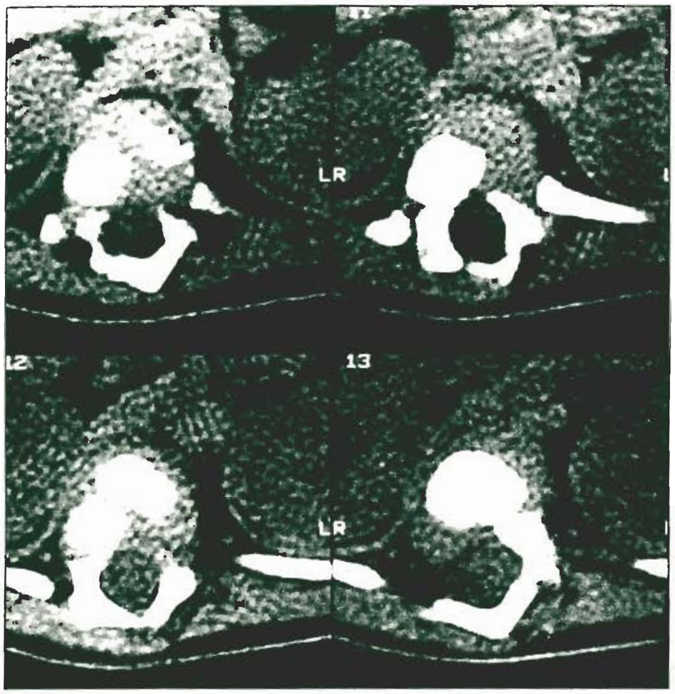

*FIGURE 7. **Posterior hemivertebra. Axial CT at the thoracolumbar junction (figure 7) sections portions of two adjacent vertebral bodies simultaneously. The spinal canal is deformed on the left.***

the original tomographic data provides an extremely precise estimate of the surface normal.

Clinical results

It must be emphasized that 3D-CT is an adjunct to axial CT. It does not yield new data; rather, it displays the data in a different manner. However, because we live in a three-dimensional world, we most readily appreciate the nuances of a complicated object if the image is presented in a three-dimensional format. The complex nature of the spine makes it an ideal subject for study with 3D-CT. Additionally, many clinicians find 3D images easier to comprehend. A significant advantage of this technology is the ability to rotate the image in order to view it from different perspectives. Frequently, this allows new insights into the morphology of the disease process.

Developmental abnormalities: Cervical spine

• *Klippel-Feil Syndrome*—Klippel-Feil syndrome is a clinical triad that consists of a short neck, restriction of cervical motion, and a low posterior hairline. This is caused by fusion of one or more cervical vertebrae. The fusion involves both the vertebral bodies and the posterior elements. Between 25% and 40% of patients with this syndrome have elevation and medial rotation of one of the scapulae.[4] This may or may not be related to the presence of an anomalous (omo-vertebral) bone. The following case illustrates how difficult it can be to evaluate this anomaly with plain radiographs and how 3D-CT can be of use in studying these patients.

This eight-month-old girl has congenital torticollis. Her neck has been deviated to the left since birth. Her left scapula also has been elevated and medially rotated. Radiographs of her cervical spine (figure 1) do not adequately evaluate the number and alignment of the cervical vertebrae. The Sprengel's deformity of the left scapula is readily apparent.

To more fully evaluate the child's cervical anomaly, three-dimensional CT was performed (figure 2). The 3-D images more clearly demonstrate the extent of cervical fusion. The degree of fusion of the vertebral bodies and the posterior elements is most readily appreciated on the midline sagittal sections.

• *Diastrophic Dwarfism*—Diastrophic dwarfism is an autosomal-recessive skeletal dysplasia that consists of a short-limbed dwarfism, club feet, scoliosis, abduction of the thumbs ("hitchhiker" thumbs) and other skeletal abnormalities. Kyphosis of the cervical spine is an inconstant feature of this dysplasia.[5]

This four-year-old boy has the classic stigmata of diastrophic dwarfism. He presented with signs of central cord syndrome, which followed minor trauma to his neck. Radiographs of the cervical spine demonstrated a marked cervical kyphosis.

To more fully evaluate the cervical spine, axial CT of the upper cervical spine section was performed through three cervical vertebrae simultaneously. In the lower cervical region, marked foreshortening of the AP diameter of the cervical canal is seen. The posterior elements of the cervical vertebrae are open (figure 3). The 3D-CT images more clearly depict the degree of spina bifida of C3 through C7. The degree of spinal stenosis and severe kyphosis in the midcervical region is most clearly seen on the midline sagittal section (figure 4).

Developmental abnormalities: Lumbar spine

• *Tethered Cord with Lipoma*—The association of fatty masses with spina bifida is common. The incidence of this association varies from 40% to 78% in various series. The lesion presents as a diffuse subcutaneous mass that has a deceptively benign appearance; it even may be cov-

A B

*FIGURE 8. **3D-CT, viewed slightly from above and from in front (figure 8A), and a midline sagittal section (figure 8B) viewed toward the patient's right, shows the left pedicle of T12 to be hypoplastic and the left half of the vertebral body to be absent. There is a rotatory dextroscoliosis. The right half of the T12 vertebral body is displaced posteriorly at the apex of the gibbus at the thoracolumbar junction.***

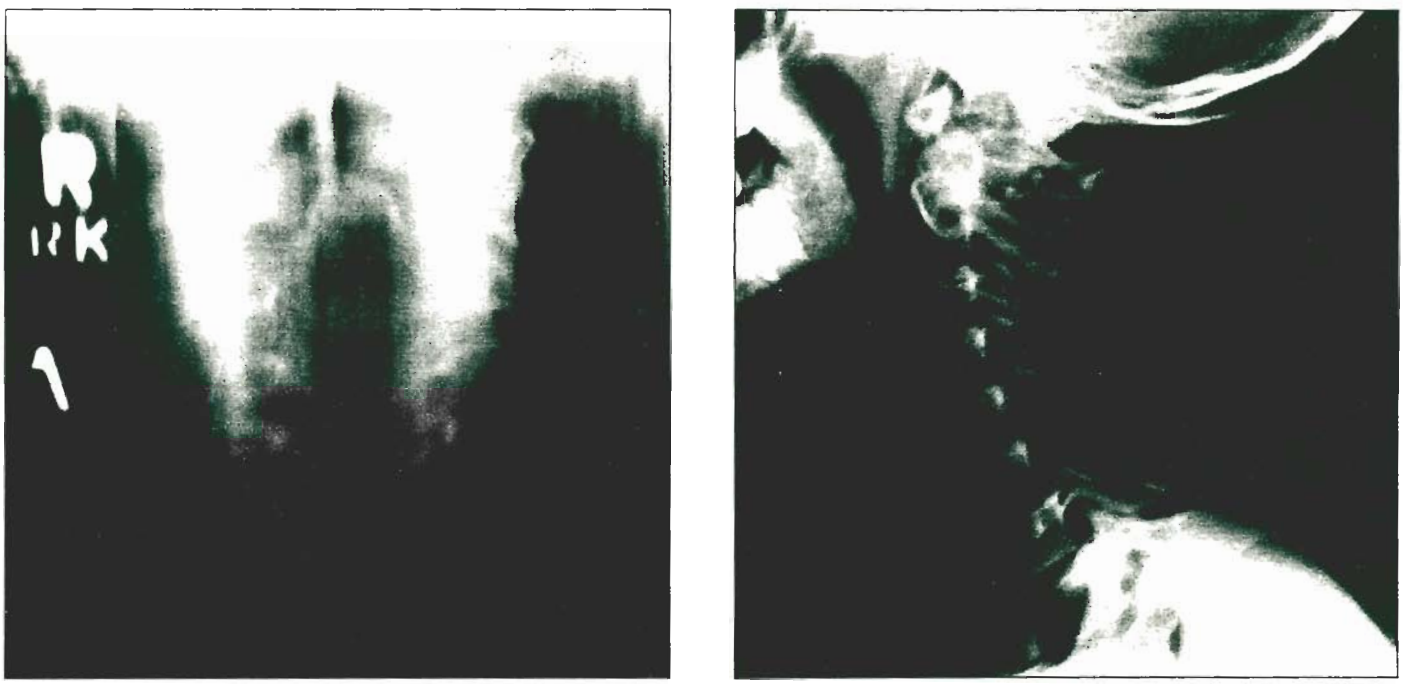

A B

*FIGURE 9. **Os odontoideum. An AP tomogram (figure 9A) and a lateral radiograph of the cervical spine (figure 9B) show the odontoid process of C2 to have a blunted and rounded appearance.***

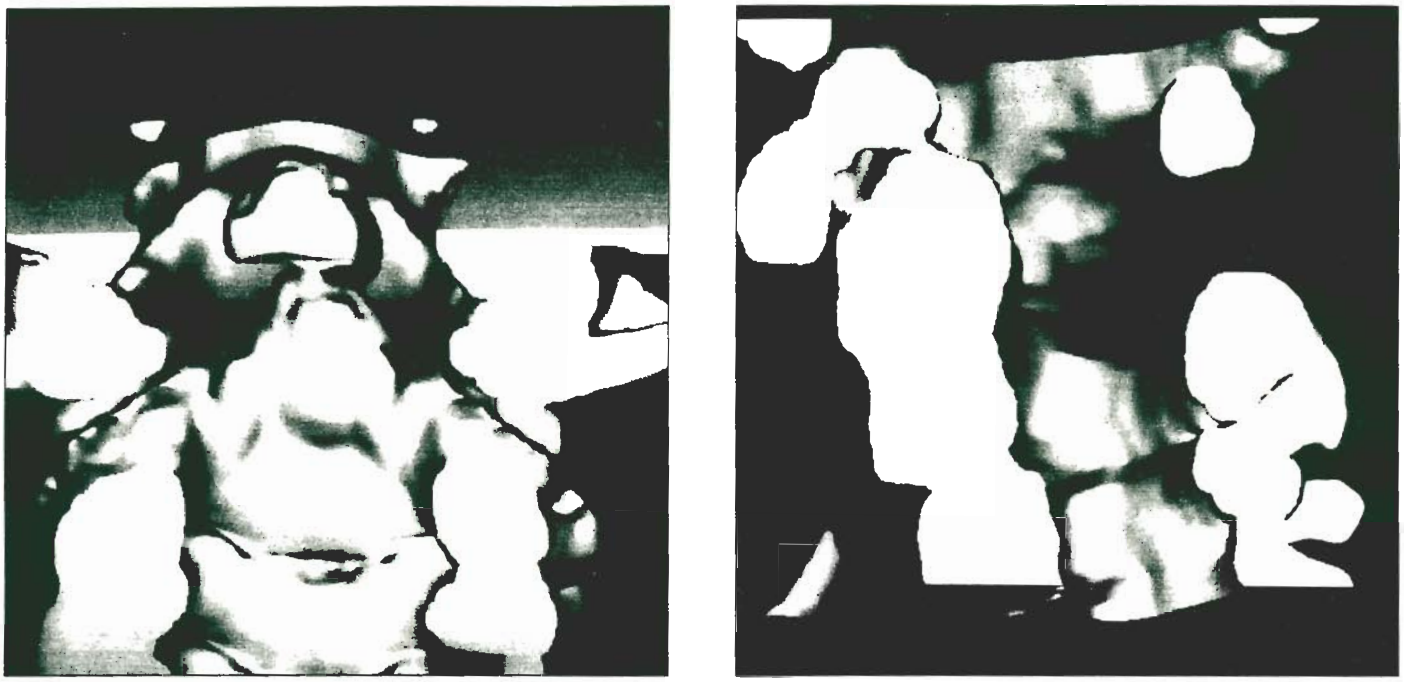

A

B

FIGURE 10. ***A coronal 3D-CT (figure 10A) is viewed from in front and slightly above. This section is approximately through the level of the pedicles of the vertebrae. The midline sagittal section (figure 10B) is viewed looking toward the patient's right. The 3-D images show a separate ossicle, an os odontoideum, which lies above and behind the posterior surface of the arch of C1; it lies just superior to the blunted dens.***

ered by normal skin. More commonly, however, there are cutaneous abnormalities such as a nevus, a dimple, or abnormal hair. The lipoma extends from the subcutaneous tissues to the intradural tissues to become attached to a thickened filum terminale. The spinal cord is usually tethered.[6]

This two-year-old girl had a fatty mass in her lower lumbar region since birth. The overlying skin was normal, and she was neurologically intact.

Following myelography, axial CT was performed. This demonstrates dysraphic changes in the lower lumbar and upper sacral regions. The spinal cord extends to the L4 level. The filum terminale is thickened and lies to the left of the midline. There is fat within the spinal canal that extends posteriorly and slightly to the right to merge with the subcutaneous fat (figure 5).

The 3D-CT images (figure 6) more clearly depict the dysraphic changes in the lower lumbar spine and sacrum. A defect is seen in the contrast-filled subarachnoid space, through which the lipoma protrudes. However, the fatty nature of the mass and the tethering of the filum terminale are not apparent on the 3D-CT images.

• *Posterior Hemivertebra*—A hemivertebra is an anomaly of vertebral segmentation. Either one-half of a vertebral body has failed to develop or there is a supernumerary half vertebra. Failure of development of the anterior half of the vertebral body results in a dorsal or posterior hemivertebra. This usually leads to a rapidly progressive kyphoscoliosis.[7]

This eight-month-old boy had a progressive thoracolumbar kyphoscoliosis. Radiographs of the spine demonstrated a hemivertebra at the T12, with a gibbus at the thoracolumbar junction.

Axial CT at the thoracolumbar junction sectioned portions of two adjacent vertebral bodies. The spinal canal is deformed (figure 7). The 3D-CT images demonstrate the left half of the T12 vertebral body to be absent and the left pedicle of T12 to be hypoplastic. The right half of the T12 vertebral body is small, and it is displaced posteriorly at the apex of the gibbus at the thoracolumbar junction (figure 8).

Traumatic lesions: Cervical spine

• *Os Odontoideum*—The os odontoideum is considered by many to be an acquired lesion that is the result of a fracture of the odontoid process of C2. Changes in the shape of the fractured segments of the odontoid have been attributed to an interference with the blood supply to the dens following the injury. These fragments usually assume a rounded appearance; they also usually maintain a relationship to the body of C1, probably due to the integrity of the posterior transverse ligaments.[8]

Three years earlier, in a car accident, this 8-year-old boy sustained an injury to his neck. At that time, radiographs of his cervical spine were normal. Recently, he has had mild discomfort in his neck.

An AP tomogram and lateral radiograph (figure 9) of the cervical spine show the odontoid to have a blunted and rounded appearance. The 3D-CT images in coronal and sagittal planes show a separate ossicle, an os odontoideum that lies above and behind the posterior surface of the arch of C1. It lies just above the blunted tip of the dens (figure 10).

Continued

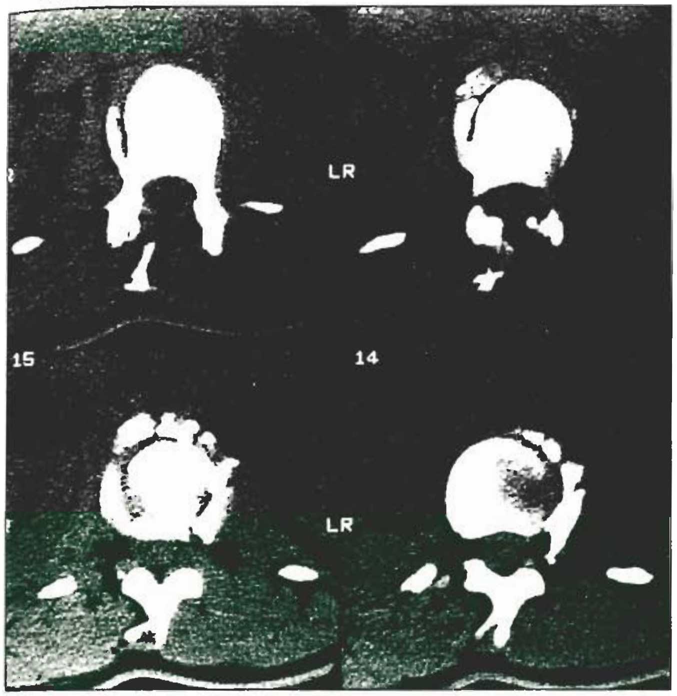

FIGURE 11. ***Complex vertebral fracture. Axial CT through the T12 vertebral body (figure 11) shows numerous fragments of the vertebral body anteriorly and to the left. There is a unilateral naked facet sign on the left.***

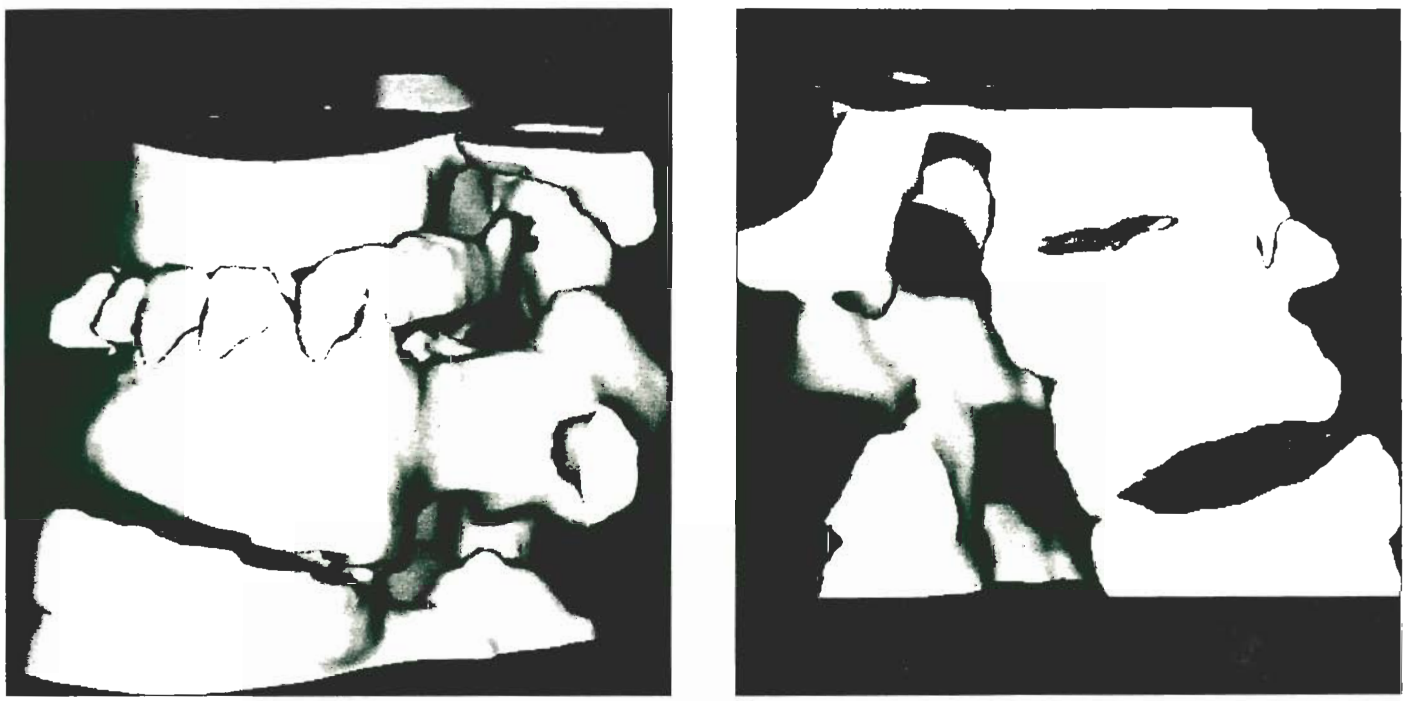

A

B

FIGURE 12. ***A steep left posterior oblique 3D-CT view of the thoracolumbar junction (figure 12A) is viewed slightly from above and towards the patient's right. There are numerous "burst" fragments arising from the superior surface of T12. One fragment has been retropulsed and it protrudes into the left T11-T12 neural foramen. The midline sagittal section (figure 12B) is viewed towards the patient's left. There are no fragments of bone within the spinal canal. The inferior articular facet of T11 is naked.***

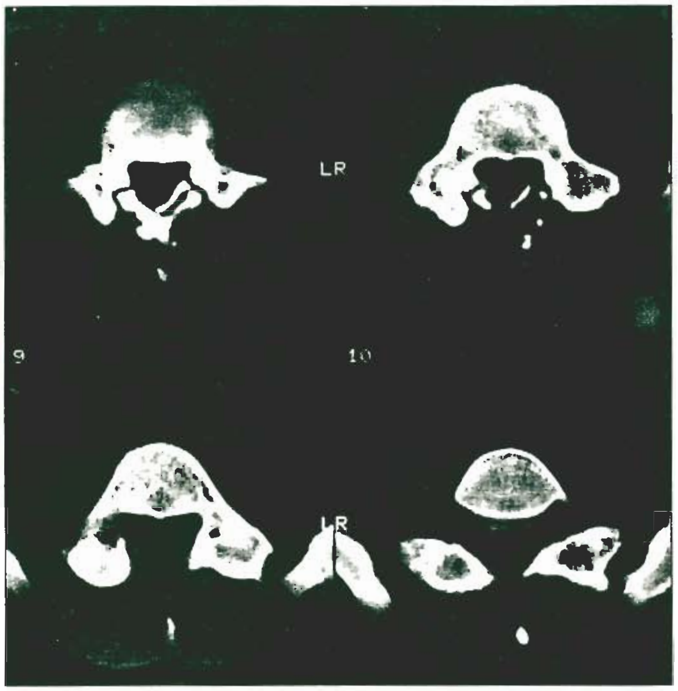

FIGURE 13. ***Postoperative complication. Axial CT through L5 (figure 13) demonstrates a large laminectomy defect. There are several fragments of bone in the spinal canal on the left.***

A

B

FIGURE 14. ***3D-CT of the lumbosacral junction (figure 14A), viewed slightly from above and from behind. The laminectomy defect and spinal fusion are readily apparent. The sagittal posterior oblique view (figure 14B) is viewed towards the patient's left. A fragment of bone is seen within the spinal canal just above the left L5-S1 neural foramen.***

Traumatic lesions: Thoracolumbar spine

• *Complex Vertebral Fracture*—Fractures at the thoracolumbar junction account for about 40% of the vertebral fractures that cause neurologic deficits. Fractures at this level are frequently complex in nature, with involvement of both the body and the posterior elements. The abnormalities of the posterior elements include diastasis of the apophyseal joints, disruption of the interspinal ligaments, and retropulsion of fragments of the body into the spinal canal.[9]

This 16-year-old girl was a passenger in an automobile that was involved in a head-on collision. She sustained a simultaneous flexion and rotation injury at the thoracolumbar junction.

Plain radiographs demonstrated a fracture of the T12 vertebral body. Axial CT shows numerous fragments of the T12

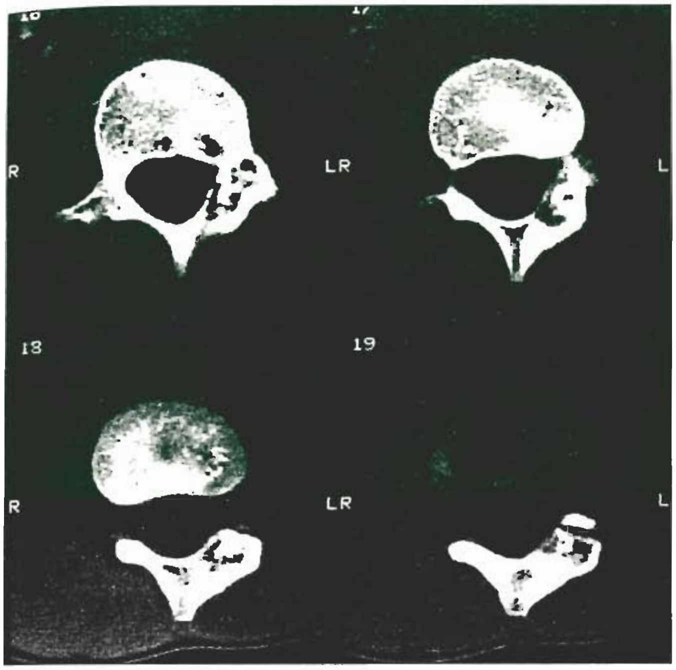

FIGURE 15. ***Osteoblastoma. Axial CT through the L2 vertebral body (figure 15) reveals an irregular expansile lesion in the left pedicle and lamina of L2 with extension into the posterior aspect of the vertebral body. The interior of the lesion contains irregular areas of calcification interspersed with mottled areas of radiolucency. The epidural space is slightly flattened on its left lateral aspect by the expansion of the lamina.***

vertebral body anteriorly. There is a unilateral naked facet sign on the left (figure 11). The 3D-CT images show numerous "burst" fragments arising from the superior surface of T12. One of the fragments has been retropulsed and protrudes into the inferior aspect of the T11-T12 neuroforamen. The midline sagittal section, viewed towards the patient's left, shows the naked facet sign. There are no fragments of bone within the spinal canal (figure 12).

• *Postoperative Complications*—Unilateral neural arch defects, with concomitant stress changes in the contralateral facet joint and pedicle, are being recognized with increasing frequency, especially among active adolescents, such as young ballet dancers and hockey players.[10]

The usual treatment for these lesions is conservative, with a prescribed period of rest to allow for healing of the neural arch defect. Those patients who fail conservative therapy usually are treated with laminectomy and spinal fusion.

In some series, up to 30% of the patients who have surgery on the lumbar spine have unsatisfactory results. Postoperative symptoms often are quite similar to the preoperative pain and radiculopathy. Axial CT has been found to be useful in evaluating the postoperative lumbar spine.[11]

This 12-year-old girl was active in ballet. She had had a prior laminectomy and spinal fusion for unilateral neural arch defect. Several months later, a radiculopathy developed.

Axial CT at the lumbosacral junction revealed a large laminectomy defect. There are several fragments of bone within the spinal canal (figure 13). Three-dimensional CT images demonstrate the laminectomy defect and, on the right, the spinal fusion. On the sagittal section, a free fragment of bone is seen within the spinal canal lying just above the left L5-S1 neural foramen (figure 14).

Neoplastic lesions

• *Osteoblastoma*—Osteoblastoma is a rare primary bone tumor that affects young persons. Approximately 55% of these lesions occur in the second decade of life. There is a significant male preponderance. From 30% to 40% of these lesions arise in the spine. Of these, about 60% are found within the posterior elements; 25% are found in the posterior elements and adjacent vertebral body; and about 15% are found solely within the vertebral body.

Radiographically, an osteoblastoma is a partially radiolucent expansile lesion that contains a variable amount of dense amorphous bone. The center of the lesion contains stippled or ringlike opaque densities.[12]

This ten-year-old boy had a three-month history of back pain that was worse at night and was partially relieved by aspirin. Radiographs of the lumbar spine revealed sclerosis of the left pedicle of L2.

Axial CT through the L2 vertebral body and posterior elements demonstrates expansion of the left pedicle and lamina of L2, with extension of the process into the left posterior aspect of the L2 vertebral body. There is a slight flattening of the left lateral aspect of the epidural space at this level (figure 15).

Three-dimensional CT confirms the expansion of the left posterior elements of L2; however, the internal characteristics of this osteoblastoma are better evaluated with axial CT (figure 16).

Conclusion

Three-dimensional CT is very helpful in studying the spine, especially if the spine is distorted by angular deformities. It is best suited for assessing osseous rather than soft-tissue abnormalities, and it is an adjunct to axial CT; it does not provide new data, but it displays the data in a different manner. A significant advantage of 3D-CT is the ability to rotate the image

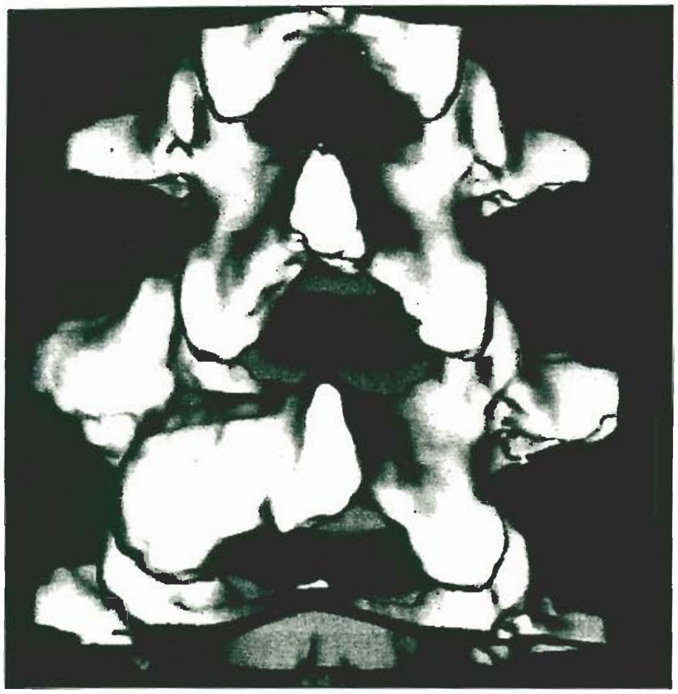

A

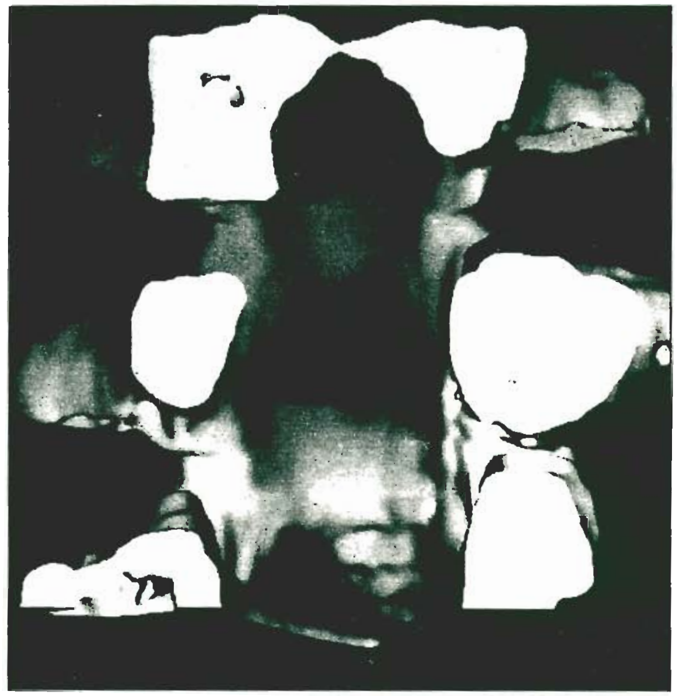

B

*FIGURE 16. **3D-CT is viewed slightly from below (figure 16A), and a coronal section through the level of the pedicles (figure 16B) is viewed slightly from below and from the front. These images confirm the expansion of the left posterior elements of L2. However, the internal features of this osteoblastoma are better characterized with axial CT.***

to any possible direction to view the object under study from different perspectives. Frequently, this allows new insights into the disease process. *AR*

References

1. **Altman NR, Altman DH, Wolfe SA, et al:** Three-dimensional CT reformation in children. AJNR 7:287–293, 1986.
2. **Vannier MW, Marsh JL, Warren JO:** Three-dimensional CT reconstruction images for craniofacial surgical planning and evaluation. Radiology 150:179–184, 1984.
3. **Cline HE, Lorensen WE, Ludke S, et al:** High resolution 3D reconstruction of tomograms. Med Phys (submitted for publication).
4. **Hensinger RN, Lang JE, MacEwen GD:** Klippel-Feil syndrome: Constellation of associated anomalies. J Bone Joint Surg 56A:1246–1253, 1979.
5. **Krecak J, Starshak RJ:** Cervical kyphosis in diastrophic dwarfism: CT and MR findings. Pediatr Radiol 17:321–322, 1987.
6. **Villarejo FJ, Blazquez MG, Gutierrez-Diaz JA:** Intraspinal lipomas in children. Childs Brain 2:361–370, 1976.
7. **Williams F, McCall IW, O'Brien JP, et al:** Severe kyphosis due to congenital dorsal hemivertebra. Clin Radiol 33:445–452, 1982.
8. **Ricciardi JE, Kaufer H, Louis DS:** Acquired os odontoideum following acute ligament injury: Report of a case. J Bone Joint Surg 58A:410–412, 1976.
9. **Kilcoyne RF, Mack LA:** Computed tomography of spinal fractures. Appl Radiol 16:40–54, 1987.
10. **Wilkinson RH, Hall JE:** The sclerotic pedicle: Tumor or pseudotumor? Radiology 111:683–688, 1974.
11. **Teplick JG, Haskin ME:** Computed tomography of the postoperative lumbar spine. AJR 141:865–884, 1983.
12. **McLeod RA, Dahlin DS, Beabout JW:** The spectrum of osteoblastoma. AJR 126:321–335, 1976.

November 1989
Vol 18 No 11

APPLIED RADIOLOGY®

THE JOURNAL OF MEDICAL IMAGING AND MANAGEMENT

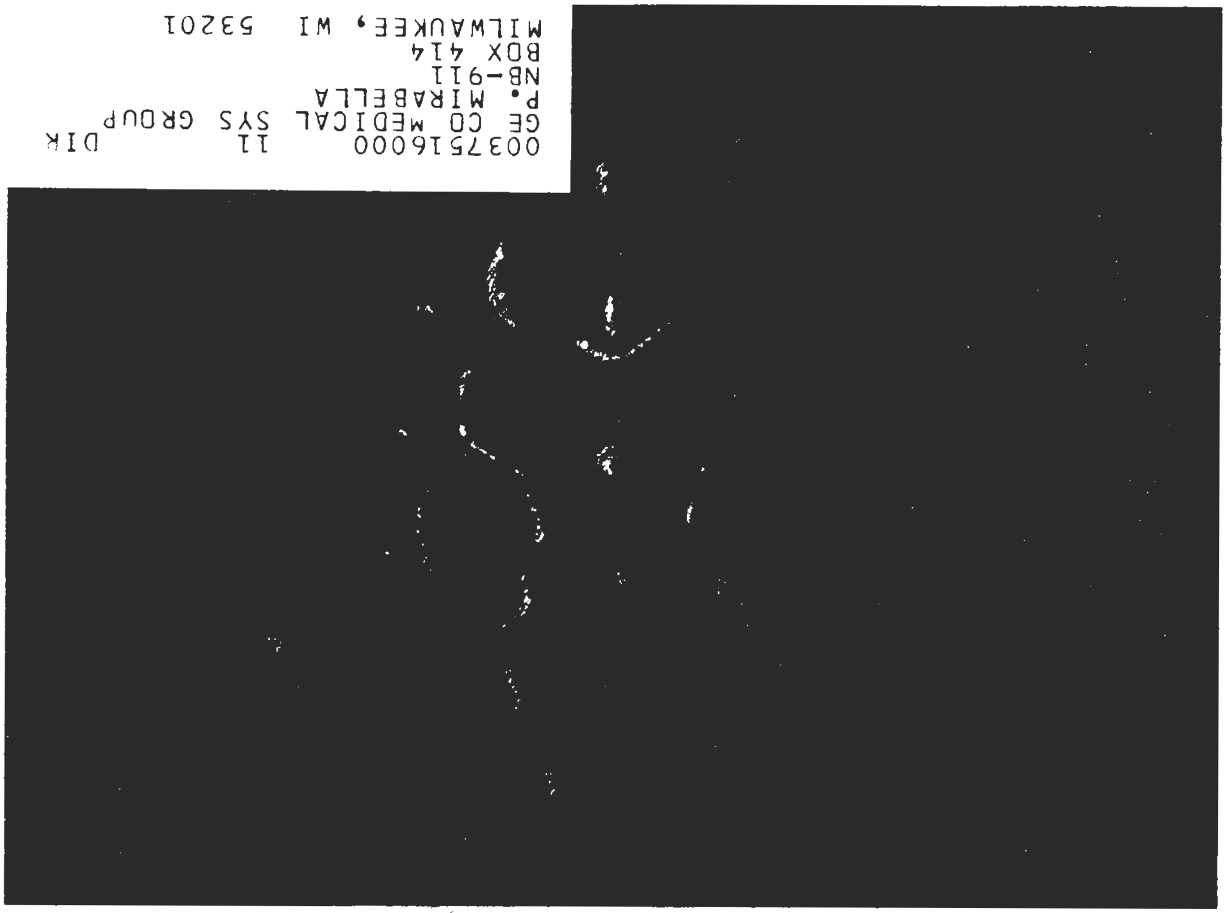

A Romaine Pierson Publication